Original article

Nuclear Medicine Communications

Diagnostic value of ^{99m}Tc-ubiquicidin scintigraphy in differentiation between osteomyelitis and bone tumors

Narjess Ayati[a], Mohammad Norouzi[a], Ramin Sadeghi[a], Mostafa Erfani[c], Mohammad Gharedaghi[b] and Kamran Aryana[a]

Aim **The differentiation of osteomyelitis from bone tumors is of great importance in clinical decision-making; however, the features of both osteomyelitis and bone tumors are noncontributory. ^{99m}Tc-ubiquicidin scintigraphy is a new promising method with the ability to specifically localize the infection site by bacterial cell membrane binding. This study aimed to evaluate the ability of this radiopeptide for the differentiation of these two entities.**

Patients and methods **Thirty consecutive patients (mean age = 20.9 years) suspected of having either osteomyelitis or bone tumor were included in this prospective study. A ^{99m}Tc-UBI scan was performed in both dynamic and static phases and the images were assessed qualitatively and semiquantitatively. The final diagnosis was established for 29 patients on the basis of surgical findings and microbiological and pathology assessments as well as any other clinical, laboratory, or imaging findings during patient follow-up.**

Results **The final diagnosis was infectious and noninfectious processes in 19 and 10 patients, respectively. Visual assessment could not distinguish between osteomyelitis and bone tumors. However, the time–activity pattern of the images proved to be promising. The sensitivity, specificity, negative and positive predictive value, and accuracy of the time–activity curve for osteomyelitis were 73.6 (54–93), 100, 66.6 (43–91), 100, and 82%, respectively. The mean ± SD tumor/nontumor (T/NT) ratios for 30 min images were 2.22 ± 0.45 and 2.02 ± 0.51 for infectious and noninfectious processes, respectively ($P = 0.29$). Using a cutoff value of 0.97 for the T/NT ratio, the sensitivity and specificity were calculated to be 78.9 and 50%, respectively.**

Conclusion **Although ^{99m}Tc-UBI scintigraphy in the dynamic imaging format was very useful with high accuracy in differentiating between infectious and tumoral lesions, it was not useful to distinguish these two entities on the basis of visual assessment or T/NT ratio measurement on static images. The study also showed the high accuracy of this noninvasive modality in acute osteomyelitis with low diagnostic value in chronic infectious processes.** ***Nucl Med Commun*** **38:885–890**

Nuclear Medicine Communications 2017, **38**:885–890

Keywords: bone tumor, osteomyelitis, ^{99m}Tc-UBI scintigraphy, ubiquicidin

[a]Nuclear Medicine Research Center, [b]Research Center of Orthopedic, Mashhad University of Medical Sciences, Mashhad and [c]Radiation Application Research School, Nuclear Science and Technology Research Institute (NSTRI), Tehran, Iran

Correspondence to Kamran Aryana, MD, Nuclear Medicine Research Center, Mashhad University of Medical Sciences, Mashhad, 9919991766 Iran
Tel: +98 513 801 2781; fax: +98 513 840 0494; e-mail: aryanak@mums.ac.ir

Received 27 May 2017 **Revised** 27 July 2017 **Accepted** 10 August 2017

Introduction

Hematogenous osteomyelitis and primary bone tumor are two important musculoskeletal pathologies whose timely diagnosis and accurate differentiation are very important in clinical medicine as a precise diagnosis affects patients' quality of life [1] and, in case of malignancy, also results in a better prognosis.

However, in the clinical setting, the differentiation of these two becomes a challenge for the clinician [2,3]. The presenting symptoms in osteomyelitis and malignant bone tumors include fever, pain, soft tissue swelling and erythema, and claudication, which are a group of nonspecific symptoms that make their differentiation difficult. Laboratory assessments are also neither specific nor sensitive enough to be useful. Even microbiologic culture has low sensitivity in osteomyelitis, with an up to 50% detection rate [4].

Similarly, radiologic modalities, despite their pivotal role in accurate diagnosis, have some limitations in certain statuses. Plain radiography is the first imaging modality for both the diseases. However, it is usually unable to differentiate them [4] simply because an infected bone lesion can appear as a radiolucent lesion with a rim of sclerosis that can be mistaken for osteosarcoma or without sclerosis, which is the presentation of Ewing's sarcoma [5]. In addition, multifocal osteomyelitis can mimic a disseminated malignancy on plain radiography [6]. Newer radiologic modalities such as computed tomgraphy and MRI can provide more detailed information that is yet again not conclusive in all situations. Recently, new signs in MRI have been suggested to distinguish between osteomyelitis and bone tumor [7]; however, the reported sensitivity is not promising.

These diagnostic limitations also exist in nuclear medicine methods such as ^{99m}Tc-MDP bone scan and gallium

0143-3636 DOI: 10.1097/MNM.0000000000000744

scintigraphy, which show tracer accumulation in both infected bones and tumor lesions [8]. However, recently, a new group of radiotracers, consisting of labeled antimicrobial peptides, has been introduced as infection imaging agents [9] including ^{99m}Tc-ubiquicidin, [(99m)Tc/Tricine/HYNIC(0)]UBI 29–41, which is a cationic synthetic peptide fragment labeled with metastable technetium, with the ability to specifically localize the infection site by binding to the bacterial cell membrane [10].

The aim of the present study is to evaluate the ability of this radiopeptide for the differentiation of osteomyelitis from primary bone tumors.

Patients and methods

This prospective study included 30 consecutive patients who were suspected to have either osteomyelitis or bone tumor in whom the clinical examination, biochemical markers, and anatomical findings in imaging studies were not diagnostically conclusive. All patients had undergone plain radiography in addition to at least one of the computed tomography or MRI of the related skeletal region that was not conclusive for a definite diagnosis. Pregnant and breastfeeding patients were excluded from the study. Following a comprehensive explanation, oral and written, of the instructions of the study and after obtaining written informed consent, a detailed assessment of medical history was performed. The patient was then scheduled for ^{99m}Tc-UBI scintigraphy. The study was approved by the ethics committee of Mashhad University of Medical Sciences (approval letter: No. 2413).

The ^{99m}Tc-ubiquicidin was prepared as described by Gandomkar *et al.* [10]. Each freeze-dried kit contained 40 μg of HYNIC-UBI 29–41, which was used for one patient. For the assessment of the radiotracer purity, thin-layer chromatography was performed and showed an average purity of greater than 95% for the radiopharmaceutical produced.

The patients were injected intravenously with 290–740 MBq of freshly prepared ^{99m}Tc-UBI. Immediate dynamic acquisition was performed using a dual-head gamma camera (E-cam; Siemens, Malvern, Pennsylvania, USA) equipped with a low-energy high-resolution parallel-hole collimator. The acquisitions were performed using a 128×128 matrix and a 20% window centered on 140 keV in the supine position aimed in the anterior–posterior direction 1 min/frame images for 30 min. Upon completion of the dynamic study, multiple 3-min spot views from the same regions were acquired. A whole-body imaging was also performed to assess the thyroid and stomach tracer uptake for quality control assurance and to assess the tracer accumulation pattern throughout the body in general.

Two experienced nuclear medicine physicians, who were blinded to patients' medical history and their previous medical data, interpreted the scans independently using qualitative and semiquantitative methods. Image processing began with a global evaluation of acquired images. The qualitative assessment included visual comparison of tracer intensity between the affected and the contralateral side. For semiquantitative evaluation, the dynamic series of images were analyzed by drawing appropriate regions of interest on the target (affected limb) and nontarget (contralateral side) regions. The time–activity curves were produced in anterior and posterior images for both areas. The semiquantitative approach was also repeated for static 30-min post-injection images.

Active follow-up was performed for all patients and the final diagnosis was established on the basis of surgical findings and microbiological and pathology assessments as well as any clinical, laboratory, or imaging findings during patient follow-up.

Statistical analyses were carried out using SPSS, version 11.5; SPSS Inc., Chicago, Illinois, USA. Quantitative variables were expressed as mean ± SD. An independent-sample *t*-test was used for comparison of quantitative variables between groups. Diagnostic indices (sensitivity, specificity, negative and positive predictive values, and accuracy) were calculated using a 2×2 table. Receiver operating characteristic curve analysis was used for the evaluation of overall accuracy of the semiquantitative approach of ^{99m}Tc-UBI scintigraphy.

P values less than 0.05 were considered statistically significant.

Results

Among the 30 consecutive patients, one refused to remain in the study after ^{99m}Tc-UBI scintigraphy and was lost to follow-up. Consequently, 29 patients (20 males) aged 3–53 years old (mean ± SD = 20.9 ± 14.3) suspected of having either osteomyelitis or bone tumor were included in our study.

The final diagnosis was infectious and noninfectious process in 19 and 10 patients, respectively. Among the 19 patients with confirmed infection, 14 had acute and five had chronic osteomyelitis. Eleven patients with bone infection had a positive microbiological culture. The final diagnosis in the remaining eight cases with negative culture was confirmed by surgical and/or pathology findings and clinical status during follow-up.

Twenty-eight out of 29 patients had positive scans by visual assessment. The experts could not distinguish patients with osteomyelitis because of noninfectious causes by visual analysis. Figure 1 shows ^{99m}Tc-UBI scintigraphy of two patients with and without bone infection.

Time–activity curve of the first 30-min dynamic acquisition showed two different patterns. In the first pattern,

Fig. 1

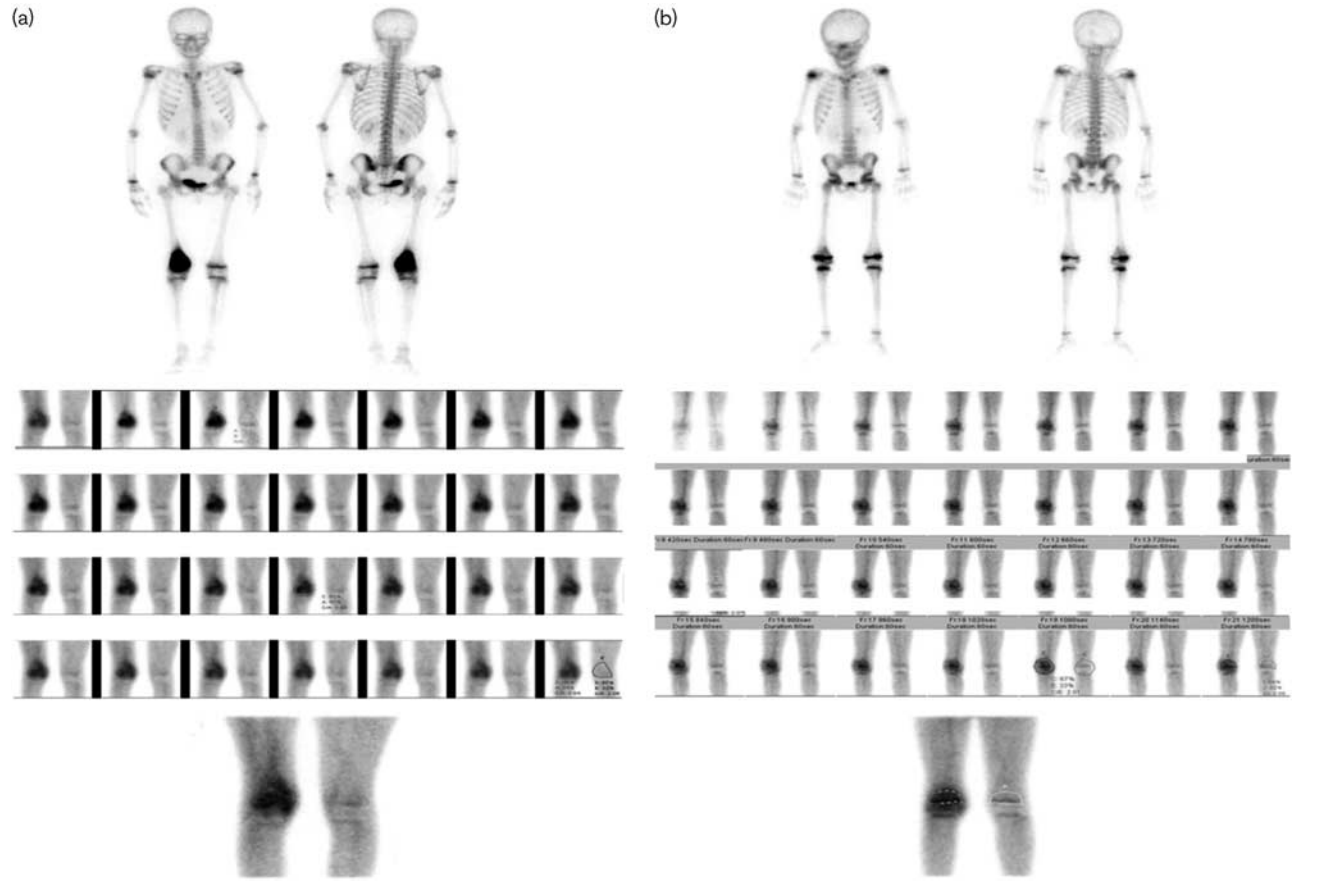

^{99m}Tc-MDP and ^{99m}Tc-ubiquicidin scintigraphies in two patients with bone lesion in the distal part of the right femur. Top row: whole-body ^{99m}Tc-MDP bone scan; Middle row: dynamic phase of ^{99m}Tc-ubiquicidin scintigraphy; Bottom row: 30 min-static image of ^{99m}Tc-ubiquicidin scintigraphy in the anterior view. (a) A 15-year-old female with right lower limb pain from 1 month ago, normal CBC, ESR = 77; T/NT at 30 min after injection: 1.95; postsurgical pathology confirmed conventional osteosarcoma. (b) A 9-year-old male with right knee pain for 1 month, Normal CBC, ESR = 23; T/NT at 30 min postinjection: 2; postsurgical pathology confirmed *Staphylococcus aureus* osteomyelitis. CBC, complete blood count; ESR, erythrocyte sedimentation rate; T/NT, tumor/nontumor, ^{99m}Tc-MDP, ^{99m}Tc-methylene diphosphonate.

the curve was slowly growing to the maximum count and remained in plateau until the end of the study (30 min). In the second pattern, the diagram showed an up-surging curve reaching the maximum count fast, but beginning to decrease over time before the end of dynamic acquisition. Figure 2 shows the two different patterns of time–activity curves.

According to the final diagnoses, all patients with acute osteomyelitis (14 cases) and one patient with chronic osteomyelitis had the first pattern and the second pattern was found in all patients without infection (10 cases) and in four out of five patients with chronic osteomyelitis. Using the time–activity pattern to differentiate between infectious and noninfectious processes, the sensitivity, specificity, negative and positive predictive values, and accuracy of the ^{99m}Tc-UBI scan for bone infection diagnosis were 73.6 (54–93), 100, 66.6 (43–91), 100, and 82%, respectively. All false-negative results (four cases) were found in patients with a chronic infectious process.

The mean ± SD tumor/nontumor (T/NT) ratios for 30 min images were 2.22 ± 0.45 and 2.02 ± 0.51 for infectious and noninfectious processes, respectively ($P = 0.29$). The only negative UBI scan by visual assessment had a T/NT ratio of 1.3 in semiquantitative analysis and the final diagnosis was 'Chronic non-specific osteomyelitis'. Table 1 shows the T/NT ratio of different noninfectious pathologies in detail.

Figure 3 shows the receiver operating characteristic curve analysis of the study. The area under the curve was 0.61 (95% confidence interval: 0.38–0.83), $P = 0.335$. Using a cutoff value of 0.97 for the T/NT ratio, the sensitivity and specificity were calculated to be 78.9 and 50%, respectively (Table 1).

Fig. 2

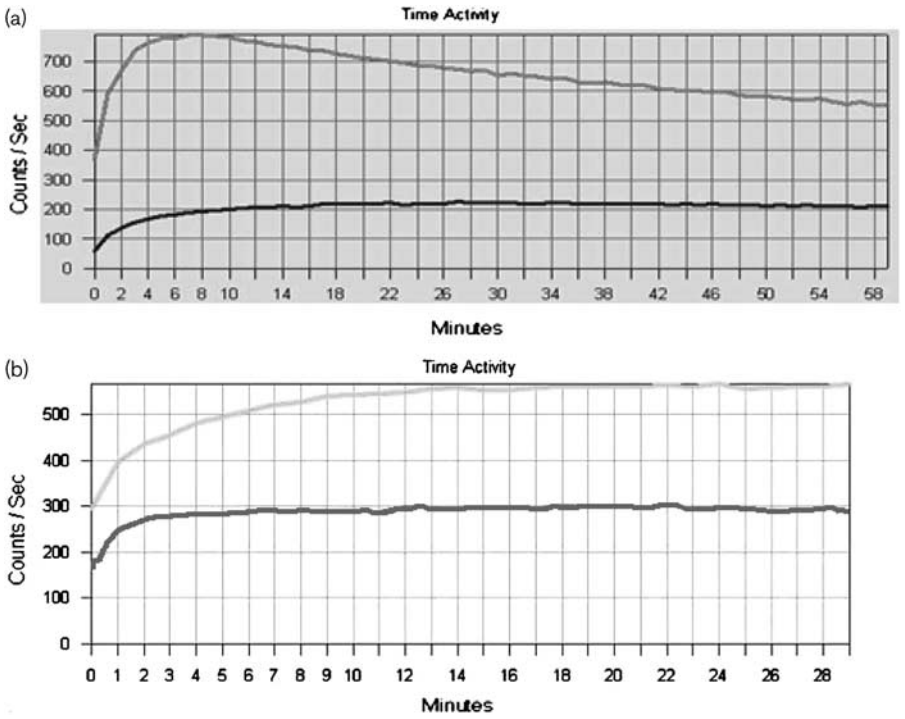

Time–activity curve in same patients presented in Fig. 1. (a) Osteosarcoma: the top image shows a rapid tracer accumulation in the affected limb, followed by a down-slope pattern only 10 min after tracer injection. The tracer activity in the contralateral side increased gradually within the first 6 min and then leveled off to the end of the study. (b) Active osteomyelitis: the curve is slowly growing to the maximum count and remained in the plateau until the end of the study (30 min). The mirror side shows a pattern similar to the contralateral side of the top image.

Table 1 Final diagnosis and tumor/nontumor ratio of patients with bone tumor

Sex	Age (years)	Final diagnosis	T/NT ratio
F	16	Osteosarcoma	2.56
M	24	Osteosarcoma	3.00
F	10	Osteosarcoma	1.59
M	53	Osteosarcoma	2.77
F	15	Osteosarcoma	1.95
F	25	Giant cell tumor	2.30
F	31	Giant cell tumor	1.45
M	4	Bone metastasis (neuroblastoma)	1.53
F	12	Ewing sarcoma	1.35
F	9	Osteoid osteoma	1.33

F, female; M, male; T/NT, tumor/nontumor.

Discussion

Nowadays, the mortality and disability rates of osteomyelitis have been reduced significantly because of new generations of antibiotics and the use of modern surgical techniques; however, the clinical approach to this pathology is still challenging for clinicians in many aspects [11]. Recent advances in radiotracer production are a promising means to deal with this dilemma in clinical encounters.

Fig. 3

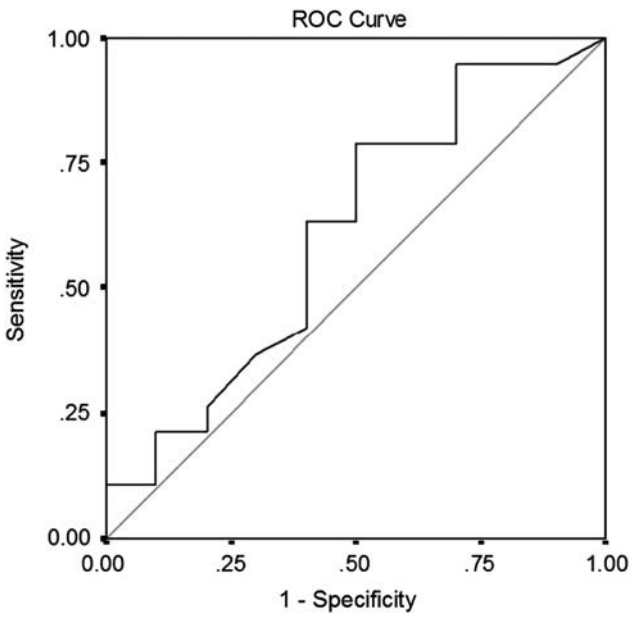

Receiver operating characteristic (ROC) curve analysis.

^{99m}Tc-UBI scintigraphy is a new promising method, with the ability to specifically localize the infection site by bacterial cell membrane binding [12]. Previous studies have indicated that this modality is capable of distinguishing between infection and sterile inflammation [13–16]. In a recent study, the researchers reported perfect sensitivity and specificity of a ^{99m}Tc-UBI scan for differentiation between prosthesis loosening and periprosthetic infection [14]. A meta-analysis on the diagnostic value of ^{99m}Tc-UBI scintigraphy in infectious process reported a sensitivity and a specificity of 94.5 and 92.7% for this modality with a 93.7% overall accuracy [17]. Theoretically, this antimicrobial peptide does not accumulate in tumor foci and it is expected that it can differentiate osteomyelitis from bone tumors. However, to our knowledge, there is no published study on this and this is the first study to compare ^{99m}Tc-UBI scan in infectious and tumoral processes.

Our study showed that tumoral tissue has the ability to show ^{99m}Tc-UBI accumulation similar to infectious lesions. Therefore, the visual assessment of images by experts could not help to differentiate between infectious and noninfectious processes. In addition, the quantitative analysis of tracer activity also could not differentiate between these two entities. In fact, the count density of radiotracer in tumor foci was three times higher than the mirror site in some cases (Table 1). Previous studies achieved a range of numbers as a cutoff for differentiation between infectious and noninfectious processes. The reported cutoffs for T/NT ratios were 1.90 ± 0.11 [14], 2.10 ± 0.33 [10], 2.75 ± 1.69 [13,] and 2.18 ± 0.74 [18]. All ratios were achieved from acquired 30-min postinjection images, except for the last study, which assessed the ratio on 2-h images. Our data showed a T/NT ratio mean of 2.22 ± 0.45 in osteomyelitis cases that was similar to the T/NT ratios of previous studies; however, the remarkable finding was the T/NT ratio of tumoral lesions (2.02 ± 0.51), which was not significantly different from infectious areas ($P > 0.05$), This result shows that despite the usefulness of the T/NT cutoff measurement as a marker of the infection process in some entities such as periprosthesis infection diagnosis, T/NT ratio assessment is not useful when the clinical aim is to distinguish osteomyelitis from bone malignancies.

The dynamic imaging showed a strong ability for this purpose by focusing on the accumulation pace. The two main patterns of tracer accumulation could accurately distinguish between acute osteomyelitis and tumoral bone lesions; however, most of the patients with chronic osteomyelitis (four out of five cases) had an accumulation pattern similar to tumoral cases with reduced tracer density in the target site before 30 min. The rational explanation for the rapid accumulation of the tracer in tumoral lesions could be hypervascularity of the region. As there is no microorganism to fix the tracer, it does not remain in the area and begins to leave the tissue without any binding. This can explain the down-slope pattern of the tracer activity.

Although the study showed a high accuracy of this modality in acute osteomyelitis, the results in chronic osteomyelitis were not promising, with a significant number of false-negative cases that resulted in reduced overall sensitivity and negative predictive value of the ^{99m}Tc-UBI scan to 73.6 and 66.6%, respectively. If only acute osteomyelitis cases are considered in the study, the sensitivity increases to 100%.

Our study was limited in several aspects. One limitation was the short duration of dynamic acquisition. Although the study showed that a ^{99m}Tc-UBI scan beyond 30 min after injection may not be necessary, static images on 60 and 120 min after injection and also continuing acquisition until the count density in the infectious area begins to reduce may be more useful. In addition, if a larger number of cases had been included in the study, categorization of osteomyelitis cases on the basis of the microorganism responsible as well as subclassification of bone tumors as benign and malignant may be possible. These issues should be studied further for better clarification.

Conclusion

Although ^{99m}Tc-UBI scintigraphy in the dynamic imaging format is promising, with over 90% accuracy in differentiation between infectious and tumoral lesions, it was not useful to distinguish these two entities on the basis of visual assessment or T/NT ratio measurement on static images. The study also showed high accuracy of this noninvasive modality in acute osteomyelitis with low diagnostic value in chronic infectious processes.

Acknowledgements

This paper is a result of a residency thesis with approval number 2633, which was supported by Deputy of Research, Mashhad University of Medical Sciences. The authors wish to thank the Vice Chancellor for Education and the Research Committee of the University for their support.

Conflicts of interest

There are no conflicts of interest.

References

1 Moser T, Ehlinger M, Chelli Bouaziz M, Fethi Ladeb M, Durckel J, Dosch JC. Pitfalls in osteoarticular imaging: how to distinguish bone infection from tumour? *Diagn Interv Imaging* 2012; **93**:351–359.
2 Love C, Palestro CJ. Nuclear medicine imaging of bone infections. *Clin Radiol* 2016; **71**:632–646.
3 Shimose S, Sugita T, Kubo T, Matsuo T, Nobuto H, Ochi M. Differential diagnosis between osteomyelitis and bone tumors. *Acta Radiol* 2008; **49**:928–933.
4 Huang PY, Wu PK, Chen CF, Lee FT, Wu HT, Liu CL, *et al.* Osteomyelitis of the femur mimicking bone tumors: a review of 10 cases. *World J Surg Oncol* 2013; **11**:283.
5 McCarville MB, Chen JY, Coleman JL, Li Y, Li X, Adderson EE, *et al.* Distinguishing Osteomyelitis From Ewing Sarcoma on Radiography and MRI. *AJR Am J Roentgenol* 2015; **205**:640–650.

6 Majd M. Radionuclide imaging in early detection of childhood osteomyelitis and its differentiation from cellulitis and bone infarction. *Ann Radiol (Paris)* 1977; **20**:9–18.

7 McGuinness B, Wilson N, Doyle AJ. The 'penumbra sign' on T1-weighted MRI for differentiating musculoskeletal infection from tumour. *Skeletal Radiol* 2007; **36**:417–421.

8 Palestro CJ. Radionuclide imaging of osteomyelitis. *Semin Nucl Med* 2015; **45**:32–46.

9 Akhtar MS, Iqbal J, Khan MA, Irfanullah J, Jehangir M, Khan B, *et al*. ^{99m}Tc-labeled antimicrobial peptide ubiquicidin (29–41) accumulates less in *Escherichia coli* infection than in Staphlococcus aureus infection. *J Nucl Med* 2004; **45**:849–856.

10 Gandomkar M, Najafi R, Shafiei M, Mazidi M, Goudarzi M, Mirfallah SH, *et al*. Clinical evaluation of antimicrobial peptide [(99m)Tc/Tricine/HYNIC(0)] ubiquicidin 29–41 as a human-specific infection imaging agent. *Nucl Med Biol* 2009; **36**:199–205.

11 Maffulli N, Papalia R, Zampogna B, Torre G, Albo E, Denaro V. The management of osteomyelitis in the adult. *Surgeon* 2016; **14**:345–360.

12 Ramin S, Narjess A, Kamran A. A pooled analysis of diagnostic value of ^{99m}Tc-ubiquicidin (UBI) scintigraphy in detection of an infectious process. *Clin Nucl Med* 2013; **38**:808–809.

13 Akhtar MS, Qaisar A, Irfanullah J, Iqbal J, Khan B, Jehangir M, *et al*. Antimicrobial peptide ^{99m}Tc-ubiquicidin 29–41 as human infection-imaging agent: clinical trial. *J Nucl Med* 2005; **46**:567–573.

14 Aryana K, Hootkani A, Sadeghi R, Davoudi Y, Naderinasab M, Erfani M, *et al*. 99m)Tc-labeled ubiquicidin scintigraphy: a promising method in hip prosthesis infection diagnosis. *Nuklearmedizin* 2012; **51**:133–139.

15 Beiki D, Yousefi G, Fallahi B, Tahmasebi MN, Gholamrezanezhad A, Fard-Esfahani A, *et al*. (99m)tc-Ubiquicidin [29–41], a promising radiopharmaceutical to differentiate orthopedic implant infections from sterile inflammation. *Iran J Pharm Res* 2013; **12**:347–353.

16 Assadi M, Vahdat K, Nabipour I, Sehhat MR, Hadavand F, Javadi H, *et al*. Diagnostic value of ^{99m}Tc-ubiquicidin scintigraphy for osteomyelitis and comparisons with ^{99m}Tc-methylene diphosphonate scintigraphy and magnetic resonance imaging. *Nucl Med Commun* 2011; **32**:716–723.

17 Ostovar A, Assadi M, Vahdat K, Nabipour I, Javadi H, Eftekhari M, *et al*. A pooled analysis of diagnostic value of (99m)Tc-ubiquicidin (UBI) scintigraphy in detection of an infectious process. *Clin Nucl Med* 2013; **38**:413–416.

18 Melendez-Alafort L, Rodriguez-Cortes J, Ferro-Flores G, Arteaga De Murphy C, Herrera-Rodriguez R, Mitsoura E, *et al*. Biokinetics of (99m)Tc-UBI 29-41 in humans. *Nucl Med Biol* 2004; **31**:373–379.